A model for ideal m=1 internal kink stabilization by minority ion cyclotron resonant heating

R. O. Dendy, R. J. Hastie, K. G. McClements, and T. J. Martin

Citation: Phys. Plasmas **2**, 1623 (1995); doi: 10.1063/1.871457
View online: http://dx.doi.org/10.1063/1.871457
View Table of Contents: http://pop.aip.org/resource/1/PHPAEN/v2/i5
Published by the American Institute of Physics.

A model for ideal $m=1$ internal kink stabilization by minority ion cyclotron resonant heating

R. O. Dendy, R. J. Hastie, K. G. McClements, and T. J. Martin
UKAEA Government Division, Fusion, Culham Laboratory (Euratom/UKAEA Fusion Association), Abingdon, Oxfordshire, OX14 3DB, United Kingdom

(Received 24 October 1994; accepted 27 January 1995)

A generalized energy principle is used to determine the effect of ion cyclotron resonant heating (ICRH) on the stability of $m=1$ internal kink displacements in the low-frequency limit: such displacements are associated with sawtooth oscillations. An integral expression is obtained for the contribution to the plasma energy of an ICRH-heated minority ion population with strong temperature anisotropy, which relates the former to the ICRH power input and its deposition profile. The link is provided by a realistic, but analytically tractable, new model for the distribution function of the heated ions, which is based on the approach of Stix [Nucl. Fusion **15**, 737 (1975)]. Numerical evaluation of the integral expression is carried out using parameters inferred from ICRH experiments in the Joint European Torus (JET) [Campbell *et al.*, Phys. Rev. Lett. **60**, 2148 (1988)]. It is shown that the ideal $m=1$ internal kink is stable at values of the poloidal plasma beta β_p which typically lie in the range 0.4–1, depending on the radio-frequency power input and the radius r_1 of the $q=1$ surface. Stability is thus possible at values of β_p lying significantly above the magnetohydrodynamic instability threshold ($\simeq 0.3$). If the perpendicular temperature $T_\perp$ of the hot ions exceeds the parallel temperature by a factor of 10 or more, and r_1 is greater than about one-third of the plasma minor radius, trapped ions have a greater stabilizing effect than passing ions. Stabilization is most easily achieved, however, if r_1 is small. The hot-ion plasma energy depends strongly on the value of $T_\perp$, but for fixed $T_\perp$ is insensitive to the degree of anisotropy.

I. INTRODUCTION

The success of experiments using minority ion cyclotron resonant heating (ICRH) to control magnetohydrodynamic (MHD) activity in the Joint European Torus (JET)[1] has given rise to considerable interest in the nature of the stabilizing mechanism, and its relation to the distribution function of the heated ions. It has been widely suggested that sawtooth oscillations are controlled by the ideal $m=1$ internal kink energy, which can be studied using MHD energy principles applied to tokamak plasma configurations. When hot minority ions are present, their potential stabilizing influence—leading, perhaps, to suppression of sawtooth oscillation—can be calculated in terms of fluid and kinetic corrections to the energy principle: these may be written in the form

$$\delta W_{\rm hot} = -\frac{1}{2}\int d^3\mathbf{r}\left(\boldsymbol{\xi}\cdot\nabla(p_\parallel+p_\perp) - (p_\parallel+p_\perp+C)\,\frac{\boldsymbol{\xi}\cdot\nabla B}{B}\right)\frac{\boldsymbol{\xi}^*\cdot\nabla B}{B} - \frac{1}{2}\int d^3\mathbf{r}\int_T d^3\mathbf{v}\left(\frac{\omega-\omega_{*h}}{\omega-\langle\omega_{dh}\rangle}\right)|\langle H\rangle|^2\,\frac{\partial F_h}{\partial \mathscr{E}}. \qquad (1)$$

Here, the key physical quantities are $\boldsymbol{\xi}$, which represents the fluid displacement associated with the MHD eigenfunction; F_h, which describes the distribution of the heated minority ions in velocity space and in real space; the minority ion diamagnetic frequency ω_{*h}; $\langle\omega_{dh}\rangle$, which is the bounce-averaged toroidal precessional drift frequency of the predominantly trapped minority ions; and $\langle H\rangle$, derived for example in Eqs. (44), (61), and (92) of Ref. 2, which is the bounce-averaged perturbed energy of a particle with fixed second adiabatic invariant J moving on magnetic field lines perturbed by the MHD eigenfunction. The quantity C is defined by Eq. (3.4) of Ref. 3, and $p_\parallel$ and $p_\perp$ refer to the parallel and perpendicular pressure of the hot ions; B denotes magnetic field strength. The integration $\int_T d^3\mathbf{v}$ is performed over trapped particles only. In Eq. (1), the first integral is referred to as the fluid term because it involves macroscopic quantities, whereas the second integral is kinetic. The latter can be derived using either the gyrokinetic equation, or methods that employ drift invariants. For further details on the derivation of the energy principle in this context, we refer for example to Refs. 2–7. It is possible to evaluate Eq. (1) for $m=1$ kink displacements, in the low-frequency limit where $\omega \ll \langle\omega_{dh}\rangle \ll \omega_{*h}$. We evaluate the contribution of passing hot ions to the fluid component of $\delta W_{\rm hot}$ in Sec. V; the total contribution of trapped ions to $\delta W_{\rm hot}$, including both fluid and kinetic terms, is given by

$$\delta W_{\rm ht} = 2^{7/2}\pi^3 m_h |\xi_{r0}|^2 \int_0^{r_1} r\,dr \int_{1/B_{\rm max}}^{1/B_{\rm min}} B_0\,d\lambda \times \int_0^\infty \mathscr{E}^{3/2}\,d\mathscr{E}\,\frac{\partial F_h}{\partial r}\left(1-\frac{\lambda B_0}{2}\right)\left(I_c - \frac{I_q^2}{I_c+sI_s}\right). \qquad (2)$$

Here, the subscript ht denotes "hot trapped"; m_h is the mi-

nority ion mass; r_1 is the minor radial coordinate of the $q=1$ surface; ξ_{r0} is the radial amplitude of the rigid-displacement eigenfunction; the magnetic field strength is defined by

$$B=B_0(1-\epsilon\cos\theta), \tag{3}$$

where $\epsilon\equiv r/R_0$ is the local inverse aspect ratio and θ denotes poloidal angle; $\mathscr{E}$ and λ are respectively energy and pitch-angle variables,

$$\mathscr{E}=v^2/2, \tag{4}$$

$$\lambda=v_\perp^2/v^2B; \tag{5}$$

the three terms I_c, I_s, and I_q are given by[8]

$$I_c=\oint\frac{d\theta}{2\pi}\frac{\cos\theta}{(1-\lambda B)^{1/2}}, \tag{6}$$

$$I_s=\oint\frac{d\theta}{2\pi}\frac{\theta\sin\theta}{(1-\lambda B)^{1/2}}, \tag{7}$$

$$I_q=\oint\frac{d\theta}{2\pi}\frac{\cos q\theta}{(1-\lambda B)^{1/2}}, \tag{8}$$

where q is the safety factor; and

$$s(r)=\left(\frac{r}{q}\right)\frac{dq}{dr}. \tag{9}$$

is the shear. When $\delta W_{\rm hot}$ is positive, the hot minority ions have a stabilizing influence. Physically, this arises[9] from the conservation of the third adiabatic invariant Φ (the flux of poloidal magnetic field through the toroidal precessional drift orbit) for minority ions with $\langle\omega_{dh}\rangle\gg\omega$. The conservation of Φ enhances the rigidity of the system, reducing the range of accessible phase space and thereby contributing to stability.

The form of Eq. (2) makes clear the crucial role of the minority ion distribution function F_h in determining the magnitude and scaling of $\delta W_{\rm ht}$. A realistic, but analytically tractable, model for F_h is therefore desirable, and this is a key feature of our calculation. In the past, three lines of approach have been followed. The first is based on the Stix distribution,[10] which predicts that the perpendicular temperature of the heated minority ion population is given by

$$T_{\perp\,\rm STIX}=T_e(1+3\xi_{\rm RF}/2),\quad \xi_{\rm RF}=\rho_{\rm RF}\tau_s/3n_hT_e. \tag{10}$$

Here, $\rho_{\rm RF}$ is the local radio-frequency (RF) power density coupled to the minority ions, τ_s is their classical Spitzer slowing-down time, T_e is the electron temperature, and n_h the number density of heated minority ions. This prediction is in broad agreement with experiment, and in particular has been used to interpret data from ICRH experiments in JET.[11,12] The RF power densities in these experiments are such that $\xi_{\rm RF}\gg1$ at the position of maximum power deposition,[11] and so $T_{\perp\,\rm STIX}\simeq3\xi_{\rm RF}T_e/2$. In the second approach, the distributions reflect geometric factors such as the cyclotron resonant localization of the heated region, and the associated "winding-up" of trapped heated particles until their banana tips lie in the heated region, which are not explicitly included in the Stix model. An example of such a distribution, which is formally more complex than the Stix model, has been given by Pegoraro and co-workers;[13] this represents an extension of the model employed by Coppi and co-workers.[7] The parameters of the model in Ref. 5 can be chosen to yield distributions having a form similar to those generated by the numerical Fokker–Planck treatment of the problem by Kerbel and co-workers,[14,15] which is representative of the third, direct numerical, line of approach.

The right-hand side of Eq. (2) contains a four-dimensional integral which must, in general, be evaluated numerically. We are faced with the challenge of finding a representation of F_h which is both realistic and sufficiently simple that the dimensionality of the integral in Eq. (2) can be reduced, thereby facilitating its numerical evaluation. In this paper we construct an expression for F_h which is analytically tractable while retaining some of the key physical features of other, more complex, approaches. In particular, it incorporates features that arise from the Stix distribution, such as the simple parametric dependence on RF power density, together with other phenomena such as the spatial localization of cyclotron resonant power deposition, and the existence of a critical pitch angle associated with banana tips lying in the heated region. This model is discussed in Sec. III, following our treatment of the poloidal and pitch-angle integrals in Sec. II, and prior to the evaluation of the trapped particle energy integral in Sec. IV. The contribution of passing hot ions to $\delta W_{\rm hot}$ is considered in Sec. V, and the model is applied to JET ICRH experiments in Sec. VI. Our conclusions are presented in Sec. VII.

II. POLOIDAL AND PITCH-ANGLE INTEGRALS

Our calculation is for minority ions that have been strongly heated and are, as a consequence, deeply trapped. It follows that $\lambda B_0\simeq1$, that in Eq. (2) we may replace $(1-\lambda B_0/2)$ by 1/2, and that in Eqs. (6)–(8) the integrations are performed between the bounce turning points at $\pm\theta_b$. Defining a new pitch-angle variable through

$$2k^2-1=(1-\lambda B_0)/\epsilon, \tag{11}$$

it follows that we may write Eq. (6) in the form

$$I_c=(2\epsilon)^{-1/2}\frac{1}{\pi}\int_0^{\theta_b}\frac{1-2\sin^2(\theta/2)}{[k^2-\sin^2(\theta/2)]^{1/2}}\,d\theta. \tag{12}$$

Using the substitution $k^2\sin^2\phi=\sin^2(\theta/2)$, this gives

$$I_c=(2\epsilon)^{-1/2}\frac{2}{\pi}[2E(k^2)-K(k^2)], \tag{13}$$

where K and E are complete elliptic integrals of the first and second kind, respectively:

$$K(k^2)=\int_0^{\pi/2}(1-k^2\sin^2\xi)^{-1/2}\,d\xi, \tag{14}$$

$$E(k^2)=\int_0^{\pi/2}(1-k^2\sin^2\xi)^{1/2}\,d\xi. \tag{15}$$

A similar approach to Eq. (7) yields, on integrating by parts,

$$I_s=(2\epsilon)^{-1/2}\frac{4}{\pi}\int_0^{\theta_b}\left[k^2-\sin^2\left(\frac{\theta}{2}\right)\right]^{1/2}d\theta, \tag{16}$$

$$=(2\epsilon)^{-1/2}\frac{8}{\pi}[(k^2-1)K(k^2)+E(k^2)]. \tag{17}$$

In order to render Eq. (8) analytically tractable, we restrict attention to the case $|q-1|\ll 1$ and Taylor expand to first order about $q=1$. This gives

$$I_q=I_c+(1-q)I_s, \tag{18}$$

where I_c and I_s are now given by Eqs. (13) and (17). Referring back to Eq. (2), we may use the above expressions to define

$$I_c-\frac{I_q^2}{I_c+sI_s}=(2\epsilon)^{-1/2}\frac{2}{\pi}H[k^2;q(r),s(r)], \tag{19}$$

where, suppressing the arguments of q and s for conciseness,

$$H(k^2;q,s)=2E(k^2)-K(k^2)-\frac{\{2E(k^2)-K(k^2)+4(1-q)[(k^2-1)K(k^2)+E(k^2)]\}^2}{2E(k^2)-K(k^2)+4s[(k^2-1)K(k^2)+E(k^2)]}, \tag{20}$$

$$=\left[8\left(\frac{s}{2}-1+q\right)[2E(k^2)-K(k^2)][(k^2-1)K(k^2)+E(k^2)]-16(1-q)^2[(k^2-1)K(k^2)+E(k^2)]^2\right]$$
$$\times\{2E(k^2)-K(k^2)+4s[(k^2-1)K(k^2)+E(k^2)]\}^{-1}. \tag{21}$$

To be consistent with the approximations already employed, we may only retain terms in Eq. (21) that are leading order in s and $1-q$. The implications of this will be examined at the end of the present section.

We have now reached a stage in the calculation where the poloidal integrations appearing in Eq. (2), which themselves involve pitch-angle information characterized by λ, have been carried out and combined to give an expression Eq. (19) which depends on the new pitch-angle variable k^2, together with the q profile and shear. We note from Eq. (11) that

$$\int_{1/B_{\min}}^{1/B_{\max}}B_0\,d\lambda=4\epsilon\int_0^1 k\,dk. \tag{22}$$

Substituting Eqs. (19) and (22) into Eq. (2), we have

$$\delta W_{\rm ht}=\frac{16\pi^2 m_h|\xi_{r0}|^2}{R_0^{1/2}}\int_0^{r_1}dr\,r^{3/2}\int_0^1 dk^2\int_0^\infty d\mathcal{E}$$
$$\times\mathcal{E}^{3/2}\left(\frac{\partial F_h}{\partial r}-\frac{1}{2r}(2k^2-1)\frac{\partial F_h}{\partial k^2}\right)H(k^2;q,s), \tag{23}$$

where the function $H(k^2;q,s)$ is defined by Eq. (21). Note that in Eq. (2), $\partial F_h/\partial r$ is evaluated at constant λ, whereas $\partial F_h/\partial r$ is evaluated at constant k^2 in Eq. (23); the transformation of partial derivatives follows from the radial dependence of k^2 at constant λ in Eq. (11). Clearly, the key physics of cyclotron resonance heating enters Eq. (23) through whatever model for F_h we choose to represent the heated minority ions. We shall address this question in the next section. Before doing so, however, there remains one outstanding point: the existence of an imaginary part of $\delta W_{\rm ht}$, in addition to the real part.

When the denominator of Eq. (21) passes through zero, the resulting pole in the k^2 integral contributes an imaginary part to $\delta W_{\rm ht}$. The term proportional to s in the denominator does not contribute to the part of Im $\delta W_{\rm ht}$ that is leading order in s over most of the range of k^2, and may therefore be neglected except when $k^2\simeq k_c^2$, where we define k_c^2 to be the root of

$$2E(k_c^2)-K(k_c^2)=0; \tag{24}$$

from standard tables, we find that $k_c^2\simeq 0.83$. Near its pole, the denominator can be expanded as $(k^2-k_c^2)$ times its first derivative with respect to k^2, evaluated at k_c^2. Using the identities

$$2K'(k^2)=\frac{E(k^2)}{k^2(1-k^2)}-\frac{K(k^2)}{k^2}, \tag{25}$$

$$2E'(k^2)=\frac{E(k^2)-K(k^2)}{k^2}, \tag{26}$$

we have for arbitrary k^2

$$\frac{d}{dk^2}[2E(k^2)-K(k^2)]$$
$$=\frac{E(k^2)-K(k^2)-k^2[2E(k^2)-K(k^2)]}{2k^2(1-k^2)}. \tag{27}$$

Meanwhile, in the first term of the numerator of Eq. (21), near the pole we have

$$2E(k^2)-K(k^2)=-4s[(k^2-1)K(k^2)+E(k^2)]. \tag{28}$$

It then follows from Eqs. (21), (24), (27), and (28) that

$$\text{Im}\int dk^2\,H(k^2;q,s)$$
$$=-32\pi k_c^2(1-k_c^2)(1-q-s)^2$$
$$\times\frac{[(k_c^2-1)K(k_c^2)+E(k_c^2)]^2}{E(k_c^2)-K(k_c^2)}, \tag{29}$$

$$=-2.27\pi(1-q-s)^2. \tag{30}$$

Physically, this imaginary contribution arises from the zero-frequency Landau resonance of heated ions near the trapped–passing boundary, whose toroidal precessional drift is negligible.

Finally, we turn to the real contribution to $\delta W_{\rm ht}$ that arises from Eq. (21). Again, it is appropriate to retain only the term that is leading order in s and $1-q$. We denote the corresponding real principal part of $H(k^2;q,s)$ by

$$PH(k^2;q,s)=8\left(\frac{s}{2}-1+q\right)[(k^2-1)K(k^2)+E(k^2)]. \tag{31}$$

Thus, in performing the integrations required to obtain $\delta W_{\rm ht}$ from Eq. (23), the real and imaginary contributions from $H(k^2;q,s)$ follow from Eqs. (31) and (30), respectively:

$$\begin{aligned}\text{Re } \delta W_{\rm ht}=&\frac{128\pi^2 m_h|\xi_{r0}|^2}{R_0^{1/2}}\int_0^{r_1} dr\, r^{3/2}\left(\frac{s(r)}{2}-1+q(r)\right)\\ &\times\int_0^1 dk^2[(k^2-1)K(k^2)+E(k^2)]\\ &\times\int_0^\infty d\mathscr{E}\,\mathscr{E}^{3/2}\left(\frac{\partial F_h}{\partial r}(r,k^2,\mathscr{E})\right.\\ &\left.-\frac{1}{2r}(2k^2-1)\frac{\partial F_h}{\partial k^2}(r,k^2,\mathscr{E})\right);\end{aligned} \tag{32}$$

$$\begin{aligned}\text{Im } \delta W_{\rm ht}=&-\frac{36.4\pi^3 m_h|\xi_{r0}|^2}{R_0^{1/2}}\int_0^{r_1} dr\, r^{3/2}[1-q(r)-s(r)]^2\\ &\times\int_0^\infty d\mathscr{E}\,\mathscr{E}^{3/2}\left(\frac{\partial F_h}{\partial r}(r,k^2=k_c^2,\mathscr{E})\right.\\ &\left.-\frac{1}{2r}(2k_c^2-1)\frac{\partial F_h}{\partial k^2}(r,k^2=k_c^2,\mathscr{E})\right).\end{aligned} \tag{33}$$

To progress further, we must now consider the distribution function of the heated minority ions.

III. MODEL DISTRIBUTION

The equilibrium distribution function of the heated minority ions (subscript h) must be expressible as $F_h(\mu,\mathscr{E},r)$ where magnetic moment $\mu=v_\perp^2/2B$, kinetic energy $\mathscr{E}=v^2/2$ as before, and r is the distance from the magnetic axis—we assume circular flux-surface cross section, for simplicity. In particular

$$\left(\frac{\partial F_h}{\partial\theta}\right)_{\mu,\mathscr{E},r}=0, \tag{34}$$

where θ denotes poloidal angle. This condition is imposed by the vanishing of $v_\parallel\mathbf{B}\cdot\nabla F_h$ in the Vlasov equation.[2] It is therefore not legitimate to construct on each flux surface a distribution function of the form

$$\begin{aligned}F_h(r,v_\perp,v_\parallel)=&n_h(r)\left(\frac{m_h}{2\pi}\right)^{3/2}\frac{1}{T_\perp(r)T_\parallel^{1/2}(r)}\\ &\times\exp\left[-\left(\frac{m_h v_\perp^2}{2T_\perp(r)}+\frac{m_h v_\parallel^2}{2T_\parallel(r)}\right)\right].\end{aligned} \tag{35}$$

Although such a distribution has been considered for the modeling of other hot-ion effects in JET,[14,15] Eq. (35) in fact violates Eq. (34) because of the dependence of magnetic field strength on poloidal angle.

In developing Stix's model, we first note that the density of RF power deposition is often a complicated function of position in ICRH experiments, as shown for example in Ref. 16. If first pass absorption is strong, power deposition is concentrated in a region of roughly equal vertical and major radial extent, determined, respectively, by wave focusing and the Doppler effect; if it is weak, power deposition is concentrated about a vertical chord. Any analytical representation of $\rho_{\rm RF}$ must accordingly include sufficient degrees of freedom to give some match to experiment, while leading, via Eq. (10), to a distribution function which satisfies Eq. (34). A relatively simple model for the spatial dependence of the power deposition density P_d is given by

$$P_d(r,\theta)=P_0\exp\left[-\left(\frac{(R-R_{\rm res})^2}{\delta^2}+\frac{z^2}{\Delta^2}\right)\right]. \tag{36}$$

Here, R denotes distance from the axis of symmetry and z denotes vertical position, so that if R_0 is the major radius of the device, $R=R_0+r\cos\theta$ and $z=r\sin\theta$; δ and Δ reflect the major radial width and vertical spread of the absorption region—we shall assume $\Delta>\delta$. Note that P_d defined by Eq. (36) is a function both of radius and of poloidal angle. It would therefore be incompatible with Eq. (34) to identify P_d, as it stands, with the quantity $\rho_{\rm RF}$ in Eq. (10), unless the resulting dependence of the distribution function on poloidal angle could somehow be removed.

Following from Eq. (36), it is convenient to define a critical radius

$$r_c=|R_{\rm res}-R_0|\frac{\Delta^2}{\Delta^2-\delta^2}. \tag{37}$$

It can be shown that the peak value of the power deposition density on a given flux surface, denoted by $\hat{P}_d(r)$, is given by

$$\hat{P}_d(r)=\begin{cases}P_0\exp\left(-\dfrac{(|R_{\rm res}-R_0|-r)^2}{\delta^2}\right), & r\leqslant r_c,\\ P_0\exp\left(\dfrac{(R_{\rm res}-R_0)^2}{\Delta^2-\delta^2}-\dfrac{r^2}{\Delta^2}\right), & r\geqslant r_c.\end{cases} \tag{38}$$

For $r\leqslant r_c$, peak power deposition occurs at $\theta=0$ or π (for $R_{\rm res}\gtrless R_0$); for $r\geqslant r_c$, it occurs at $\theta=\cos^{-1}(sr_c/r)$, where $s=\text{sign}(R_{\rm res}-R_0)$.

We now make an assumption which is crucial to our model: the heated ion distribution on a flux surface will be governed by Stix's model, as evaluated at the point on the flux surface where heating is greatest. Accordingly, we identify

$$\rho_{RF}(r)=\hat{P}_d(r) \tag{39}$$

for use in Eq. (10). The distribution function may then be written in the form

$$F_h(\mu,\mathscr{E},r)=\frac{C_0(r)}{T_\perp^{3/2}(r)}\left(\frac{m_h}{2\pi}\right)^{3/2} \times\exp\left[-m_h\left(\frac{\mu B(r,\theta_0)}{T_\perp(r)}+\frac{|\mathscr{E}-\mu B(r,\theta_0)|}{T_\parallel(r)}\right)\right]. \tag{40}$$

Here (r,θ_0) denotes the point on the flux surface at which RF power deposition density is greatest;

$$T_\perp(r)=T_{\perp\ \mathrm{STIX}}(\rho_{RF}(r),n_e,T_e,n_h), \tag{41}$$

using Eqs. (10), (38), and (39); $T_\parallel(r)$ can be modeled as appropriate; and $C_0(r)$ is a normalization factor which we calculate below. In the outer midplane ($\theta=0$), F_h is sharply peaked at pitch angles lying symmetrically above and below 90° which correspond to bounce reflection at $\theta=\pm\theta_0$. Such a representation of F_h is consistent with Fokker–Planck calculations of ICRH-heated ion distribution functions (see, for example, Fig. 15 of Ref. 14 and Fig. 3 of Ref. 15).

It is convenient to denote by B_R the magnetic field strength at the position of maximum heating and, following Eq. (3), to relate B_R to a new parameter $\hat{\epsilon}$ defined by

$$B_R=B_0(1-\hat{\epsilon}). \tag{42}$$

Then, using also Eqs. (5) and (11), we may write the argument of the exponential in Eq. (40) as

$$-\frac{m_h\mathscr{E}}{T_\perp}\left(\lambda B_0(1-\hat{\epsilon})+\frac{T_\perp}{T_\parallel}|1-\lambda B_0(1-\hat{\epsilon})|\right) =-\frac{m_h\mathscr{E}}{T_\perp}\left(1+\frac{T_\perp}{T_\parallel}|\epsilon(2k^2-1)+\hat{\epsilon}|\right). \tag{43}$$

The expressions on both sides of Eq. (43) will be useful in what follows. In particular, since

$$d^3v=4\pi\frac{B}{|v_\parallel|}\,d\mu\,d\mathscr{E}=2^{3/2}\pi\frac{B\mathscr{E}^{1/2}\,d\lambda\,d\mathscr{E}}{(1-\lambda B)^{1/2}}, \tag{44}$$

we may write

$$\int d^3v\,\exp\left[-\frac{m_h\mathscr{E}}{T_\perp}\left(1+\frac{T_\perp}{T_\parallel}|\epsilon(2k^2-1)+\hat{\epsilon}|\right)\right] =2^{3/2}\pi\int\frac{B\,d\lambda}{(1-\lambda B)^{1/2}}\mathscr{E}^{1/2} \times\exp\left[-\frac{m_h\mathscr{E}}{T_\perp}\left(\lambda B_R+\frac{T_\perp}{T_\parallel}|1-\lambda B_R|\right)\right]d\mathscr{E} =2^{1/2}\pi^{3/2}\left(\frac{m_h}{T_\perp}\right)^{-3/2}I_\lambda(r,\theta), \tag{45}$$

where

$$I_\lambda(r,\theta)=\int_0^{1/B(r,\theta)}\frac{B\,d\lambda}{(1-\lambda B)^{1/2}} \times\frac{1}{[\lambda B_R+(T_\perp/T_\parallel)|1-\lambda B_R|]^{3/2}}. \tag{46}$$

It then follows from Eqs. (40), (43), and (45) that

$$\int F_h\,d^3v=\frac{1}{2}C_0(r)I_\lambda(r,\theta). \tag{47}$$

The appearance of θ in the Jacobian of Eq. (44) means that the velocity space integral of F_h is θ dependent, despite the fact that F_h itself, when expressed as a function of λ, $\mathscr{E}$, and r, is θ independent. In order to obtain an expression for $C_0(r)$ we integrate both sides of Eq. (47) with respect to θ, using the fact that

$$n_h(r)=\frac{1}{2\pi}\oint d\theta\int F_h\,d^3\mathbf{v}. \tag{48}$$

Then by Eqs. (40), (43), and (46)–(48),

$$F_h(\mathscr{E},k^2,r) =2n_h(r)\left(\frac{m_h}{2\pi T_\perp(r)}\right)^{3/2}G(r) \times\exp\left[-\frac{m_h\mathscr{E}}{T_\perp(r)}\left(1+\frac{T_\perp(r)}{T_\parallel(r)}|\epsilon(2k^2-1)+\hat{\epsilon}|\right)\right], \tag{49}$$

$$G(r)=\left(\int_0^{1/B_{\min}(r)}\frac{d\lambda}{[\lambda B_R+(T_\perp/T_\parallel)|1-\lambda B_R|]^{3/2}}\frac{1}{2\pi} \times\oint\frac{B\,d\theta}{(1-\lambda B)^{1/2}}\right)^{-1}. \tag{50}$$

In Eq. (49), recall that $\epsilon=r/R_0$, $\hat{\epsilon}$ is defined by Eq. (42), and $T_\perp(r)$ is constructed in terms of the Stix approach by the steps leading up to Eq. (41). We show in the Appendix that the normalization function $G(r)$ can be expressed in terms of elliptic integrals. In the next section, we substitute the model distribution function given by Eq. (49) into the expressions for Re δW_{ht} and Im δW_{ht} obtained at the end of Sec. II.

IV. RADIAL AND ENERGY INTEGRALS

The dependence on radial coordinate r of the model distribution function F_h defined by Eq. (49) is somewhat complicated. This makes it appropriate to carry out the radial integrations in Eqs. (32) and (33) by parts, rather than to evaluate $\partial F_h/\partial r$ explicitly. Noting that $q(r_1)=1$ by definition, we obtain the following results for use in Eqs. (32) and (33), respectively:

$$\int_0^{r_1} dr\, r^{3/2}\left(\frac{s(r)}{2}-1+q(r)\right)\frac{\partial F_h}{\partial r}$$

$$=\frac{r_1^{3/2}}{2}s(r_1)F_h(\mathscr{E},k^2,r_1)-\int_0^{r_1}dr$$

$$\times F_h r^{1/2}\left[\frac{3}{2}\left(\frac{s(r)}{2}-1+q(r)\right)+r\left(\frac{dq}{dr}+\frac{1}{2}\frac{ds}{dr}\right)\right], \quad (51)$$

$$\int_0^{r_1} dr\, r^{3/2}[1-q(r)-s(r)]^2\frac{\partial F_h}{\partial r}$$

$$=s^2(r_1)r_1^{3/2}F_h(\mathscr{E},k^2,r_1)-\int_0^{r_1}dr\, F_h r^{1/2}[1-q(r)-s(r)]$$

$$\times\left[\frac{3}{2}[1-q(r)-s(r)]-2r\left(\frac{dq}{dr}+\frac{ds}{dr}\right)\right]. \quad (52)$$

It is also useful to note that the component of the integrand in Eq. (32) that is proportional to $\partial F_h/\partial k^2$ can be transformed by integration by parts. Using Eqs. (25) and (26), we obtain

$$\int_0^1 dk^2[(k^2-1)K(k^2)+E(k^2)](2k^2-1)\frac{\partial F_h}{\partial k^2}$$

$$=F_h(r,k^2=1,\mathscr{E})-\int_0^1 dk^2$$

$$\times F_h\left[\left(3k^2-\frac{5}{2}\right)K(k^2)+2E(k^2)\right]. \quad (53)$$

We are now in a position to consider the energy integral. In doing so, we require the identity

$$\int_0^\infty t^z \exp(-\alpha t)dt=\alpha^{-(z+1)}\Gamma(z+1), \quad (54)$$

where $\Gamma(p+1)=p\Gamma(p)$ and $\Gamma(1/2)=\pi^{1/2}$. Then, from Eq. (49),

$$\int_0^\infty d\mathscr{E}\,\mathscr{E}^{3/2}F_h(\mathscr{E},k^2,r)$$

$$=\frac{3n_h(r)T_\perp(r)G(r)}{2^{5/2}\pi m_h}$$

$$\times\left(1+\frac{T_\perp(r)}{T_\parallel(r)}\left|\frac{r}{R_0}(2k^2-1)+\hat{\epsilon}\right|\right)^{-5/2}. \quad (55)$$

It follows that, for use in Eq. (33),

$$\int_0^\infty d\mathscr{E}\,\mathscr{E}^{3/2}\frac{\partial F_h}{\partial k^2}(r,k^2=k_c^2,\mathscr{E})$$

$$=-5\frac{rT_\perp(r)}{R_0T_\parallel(r)}\sigma(r)\left(1+\frac{T_\perp(r)}{T_\parallel(r)}\left|\frac{r}{R_0}(2k_c^2-1)+\hat{\epsilon}\right|\right)^{-1}$$

$$\times\int_0^\infty d\mathscr{E}\,\mathscr{E}^{3/2}F_h, \quad (56)$$

where $\sigma(r)$ is ±1 for $(r/R_0)(2k_c^2-1)+\hat{\epsilon}\gtrless 0$.

Let us now consider the normalization of $\delta W_{\rm ht}$. The simplest point of comparison is provided by the standard MHD toroidal energy,[17]

$$\delta W^{(T)}=W_0\left(\frac{13}{144}-\beta_p^2\right)[1-q(0)], \quad (57)$$

$$W_0=6\pi^2\left(\frac{r_1}{R_0}\right)^4 R_0|\xi_{r0}|^2\frac{B_0^2}{\mu_0}, \quad (58)$$

where β_p denotes the poloidal beta. Accordingly, we define

$$(\delta W_{\rm ht})_N=\delta W_{\rm ht}/W_0, \quad (59)$$

so that $(\delta W_{\rm ht})_N$ is a dimensionless number whose magnitude is to be compared to $(13/144-\beta_p^2)[1-q(0)]$. It is also convenient to define

$$\hat{n}_h=n_h/10^{19}\ \mathrm{m}^{-3}, \quad (60)$$

$$\hat{T}_\perp=T_\perp/1\ \mathrm{keV}, \quad (61)$$

$$\hat{B}_0=B_0/1\ \mathrm{T}, \quad (62)$$

so that

$$\frac{\mu_0 n_h T_\perp}{B_0^2}=2.013\times10^{-3}\frac{\hat{n}_h\hat{T}_\perp}{\hat{B}_0^2}. \quad (63)$$

Also, denoting the minor radius of the plasma by a, we define

$$x=r/a, \quad x_1=r_1/a, \quad (64)$$

$$\epsilon_a=a/R_0. \quad (65)$$

Substituting Eqs. (51)–(53), (55), and (56) into Eqs. (32) and (33), and reducing the resulting expressions to dimensionless form, we obtain

$$\mathrm{Re}(\delta W_{\mathrm{ht}})_N = 7.25\times10^{-3}\epsilon_a^{-5/2}x_1^{-5/2}\Bigg[\int_0^1 dk^2[(k^2-1)K(k^2)+E(k^2)]\,\frac{s(x_1)\hat{n}_h(x_1)\hat{T}_\perp(x_1)G(x_1)}{2\hat{B}_0^2}$$
$$\times\left(1+\frac{T_\perp(x_1)}{T_\parallel(x_1)}\,|x_1\epsilon_a(2k^2-1)+\hat{\epsilon}|\right)^{-5/2} - x_1^{-3/2}\int_0^{x_1} dx\; x^{1/2}\left(\frac{s(x)}{2}-1+q(x)\right)\frac{\hat{n}_h(x)\hat{T}_\perp(x)G(x)}{\hat{B}_0^2}$$
$$\times\left(1+\frac{T_\perp(x)}{T_\parallel(x)}\,|x\epsilon_a+\hat{\epsilon}|\right)^{-5/2} - x_1^{-3/2}\int_0^{x_1} dx\; x^{3/2}\left(\frac{1}{2}\frac{ds}{dx}+\frac{dq}{dx}\right)\frac{\hat{n}_h(x)\hat{T}_\perp(x)G(x)}{\hat{B}_0^2}\int_0^1 dk^2[(k^2-1)K(k^2)+E(k^2)]$$
$$\times\left(1+\frac{T_\perp(x)}{T_\parallel(x)}\,|x\epsilon_a(2k^2-1)+\hat{\epsilon}|\right)^{-5/2} - \frac{x_1^{-3/2}}{4}\int_0^{x_1} dx\; x^{1/2}\left(\frac{s(x)}{2}-1+q(x)\right)\frac{\hat{n}_h(x)\hat{T}_\perp(x)G(x)}{\hat{B}_0^2}$$
$$\times\int_0^1 dk^2[2E(k^2)-K(k^2)]\left(1+\frac{T_\perp(x)}{T_\parallel(x)}\,|x\epsilon_a(2k^2-1)+\hat{\epsilon}|\right)^{-5/2}\Bigg], \tag{66}$$

$$\mathrm{Im}(\delta W_{\mathrm{ht}})_N = -6.48\times10^{-3}\epsilon_a^{-5/2}x_1^{-5/2}\Bigg[\frac{s^2(x_1)\hat{n}_h(x_1)\hat{T}_\perp(x_1)G(x_1)}{\hat{B}_0^2}\left(1+\frac{T_\perp(x_1)}{T_\parallel(x_1)}\,|0.66x_1\epsilon_a+\hat{\epsilon}|\right)^{-5/2}$$
$$-\frac{3}{2}x_1^{-3/2}\int_0^{x_1} dx\; x^{1/2}\,\frac{\hat{n}_h(x)\hat{T}_\perp(x)G(x)}{\hat{B}_0^2}\,[1-q(x)-s(x)]^2\left(1+\sigma(x)\,\frac{T_\perp(x)}{T_\parallel(x)}\,(\hat{\epsilon}-0.44x\epsilon_a)\right)$$
$$\times\left(1+\frac{T_\perp(x)}{T_\parallel(x)}\,|0.66x\epsilon_a+\hat{\epsilon}|\right)^{-7/2} + 2x_1^{-3/2}\int_0^{x_1} dx\; x^{3/2}\,\frac{\hat{n}_h(x)\hat{T}_\perp(x)G(x)}{\hat{B}_0^2}\,[1-q(x)-s(x)]\left(\frac{dq}{dx}+\frac{ds}{dx}\right)$$
$$\times\left(1+\frac{T_\perp(x)}{T_\parallel(x)}\,|0.66x\epsilon_a+\hat{\epsilon}|\right)^{-5/2}\Bigg]. \tag{67}$$

Here, $\sigma(x)=\pm1$ for $x\epsilon_a(2k_c^2-1)+\hat{\epsilon}\gtrless0$. Polynomial approximations can be used to evaluate $K(k^2)$ and $E(k^2)$ rapidly, which means that the integrals in Eqs. (66) and (67) are effectively either one dimensional or two dimensional, and are thus tractable numerically.

It is also convenient to express the radial and parametric dependence of $T_\perp(r)$ in terms of suitably normalized units. If P_c is the total power coupled to the minority ion population, we may define

$$P_0 = P_c/2\pi^2R_0\Delta\,\delta \tag{68}$$

for use in Eq. (38). It then follows from Eqs. (10), (38), and (41) that

$$\hat{T}_\perp(x) = 2\left(\frac{A_h}{Z_h^2}\right)\left(\frac{n_{h0}}{n_0}\right)^{-1}\hat{n}_e^{-2}(x)\hat{T}_e^{3/2}(x)P_0$$
$$\times\begin{cases} f_1(x), & x\leqslant x_c,\\ f_2(x), & x\geqslant x_c.\end{cases} \tag{69}$$

Here, the normalizations of temperatures and density are as in Eqs. (62) and (63), P_0 is denominated in MWm^{-3}, A_h and Z_h are the atomic mass number and charge of the heated minority ions, (n_{h0}/n_0) is the minority ion concentration which is assumed independent of radius, and

$$f_1(x) = \exp\left(-\frac{(|\hat{\epsilon}|/\epsilon_a-x)^2}{\hat{\delta}^2}\right), \tag{70}$$

$$f_2(x) = \exp\left(\frac{\hat{\epsilon}^2/\epsilon_a^2}{\hat{\Delta}^2-\hat{\delta}^2}-\frac{x^2}{\hat{\Delta}^2}\right), \tag{71}$$

$$x_c = \frac{|\hat{\epsilon}|}{\epsilon_a}\,\frac{\hat{\Delta}^2}{\hat{\Delta}^2-\hat{\delta}^2}, \tag{72}$$

with $\hat{\Delta}=\Delta/a$, $\hat{\delta}=\delta/a$.

V. PASSING PARTICLE CONTRIBUTION TO THE ENERGY

While the passing component of the energetic ion population makes no contribution to the kinetic part of δW_{hot}, it does contribute to the fluid part. As we noted in the Introduction, this contribution was neglected in passing from Eq. (1) to (2), and we now evaluate it explicitly. We define

$$\delta W_{\mathrm{hfp}} = -\frac{m_h}{2}\int d^3\mathbf{r}\,\frac{\boldsymbol{\xi}^*\cdot\nabla B}{B}\int_P d^3\mathbf{v}(v_\parallel^2+\mu B)\boldsymbol{\xi}\cdot\nabla F_h, \tag{73}$$

where the subscript "hfp" denotes "hot fluid passing" and $\int_P d^3\mathbf{v}$ denotes integration over passing particles in velocity space. The trapped hot fluid contribution to δW is formally similar to Eq. (73), with $\int_P d^3\mathbf{v}$ replaced by $\int_T d^3\mathbf{v}$. When these two contributions are summed, we obtain the total fluid contribution to δW_{hot} which is given by the first integral expression in Eq. (1). This involves the total energetic particle pressures $p_\parallel$ and $p_\perp$, and the quasipressure C, which are defined by

$$p_\parallel = \int d^3\mathbf{v}\; m_h v_\parallel^2 F_h = 4\pi m_h\int\frac{B}{|v_\parallel|}\,v_\parallel^2\; d\mu\; d\mathcal{E}\; F_h, \tag{74}$$

$$p_\perp = \int d^3\mathbf{v}\left(\frac{m_h v_\perp^2}{2}\right)F_h = 4\pi m_h\int\frac{B}{|v_\parallel|}\,\mu B\; d\mu\; d\mathcal{E}\; F_h, \tag{75}$$

$$C=4\pi m_h\int \frac{B}{|v_\parallel|}(\mu B)^2\frac{\partial F_h}{\partial \varepsilon}\,d\mu\,d\mathscr{E}. \tag{76}$$

We define corresponding passing quantities $\tilde{p}_\parallel$, $\tilde{p}_\perp$, and $\tilde{C}$ for which the integrations in Eqs. (74)–(76) are restricted to the passing volume of velocity space—that is, the range $\mathscr{E}=0$ to ∞ and $\mu=0$ to $\mathscr{E}/B_{\max}$.

Returning to Eq. (73), we consider a leading-order displacement $\boldsymbol{\xi}_0$ with $m=n=1$ such that $\xi_\theta=i\xi_r$. It follows that

$$\frac{\boldsymbol{\xi}^*\cdot\nabla B}{B}=-\frac{\xi_r^*\cos\theta}{R_0}+\frac{\xi_\theta^*\sin\theta}{R_0}=-\frac{\xi_{r0}^*}{R_0}e^{i\theta}e^{-i(\theta-\phi)}, \tag{77}$$

$$\boldsymbol{\xi}\cdot\nabla F_h=\xi_{r0}e^{i(\theta-\phi)}\frac{\partial F_h}{\partial r}, \tag{78}$$

and Eq. (73) then yields

$$\delta W_{\rm hfp}=\frac{m_h}{2}\int_0^{r_1}\int_0^{2\pi}\int_0^{2\pi}\frac{rR^2}{R_0}\,dr\,d\theta\,d\phi\,\frac{|\xi_{r0}|^2}{R_0}\times\cos\theta\int_P d^3\mathbf{v}(v_\parallel^2+\mu B)\frac{\partial F_h}{\partial r}. \tag{79}$$

Here the notation for the spatial volume element follows the convention of Ref. 17. In formulating our total energy principle, $\delta W_{\rm hfp}$ will be added to $\delta W_{\rm ht}$ defined by Eq. (2) and evaluated in the preceding sections. We recall that the latter contains the trapped hot fluid and full kinetic contributions.

Evaluation of the velocity-space integrations in Eq. (79) is assisted by considering the partial radial derivatives of $\tilde{p}_\perp$ and $\tilde{p}_\parallel$, noting that B, $v_\parallel$, $B_{\max}$, and F_h are all explicit functions of r. We have

$$\frac{\partial\tilde{p}_\parallel}{\partial r}=\frac{(\tilde{p}_\parallel-\tilde{p}_\perp)}{B}\frac{\partial B}{\partial r}+\int_P d^3\mathbf{v}\,m_h v_\parallel^2\frac{\partial F_h}{\partial r}+B\frac{d}{dr}\left(\frac{1}{B_{\max}}\right)\left(1-\frac{B}{B_{\max}}\right)^{1/2}2^{5/2}\pi m_h\times\int_0^\infty\mathscr{E}^{3/2}F_h\left(\mu=\frac{\mathscr{E}}{B_{\max}},\mathscr{E},r\right)d\mathscr{E}, \tag{80}$$

$$\frac{\partial\tilde{p}_\perp}{\partial r}=\frac{(2\tilde{p}_\perp+\tilde{C})}{B}\frac{\partial B}{\partial r}+\int_P d^3\mathbf{v}\,m_h\mu B\frac{\partial F_h}{\partial r}+B\frac{d}{dr}\left(\frac{1}{B_{\max}}\right)\frac{B/B_{\max}}{(1-B/B_{\max})^{1/2}}2^{3/2}\pi m_h\times\int_0^\infty\mathscr{E}^{3/2}F_h\left(\mu=\frac{\mathscr{E}}{B_{\max}},\mathscr{E},r\right)d\mathscr{E}. \tag{81}$$

Substituting expressions from Eqs. (80) and (81) into Eq. (79), and integrating over toroidal angle ϕ, we obtain

$$\delta W_{\rm hfp}=\pi|\xi_{r0}|^2\int_0^{r_1}r\,dr\int d\theta\cos\theta\times\left\{\frac{\partial}{\partial r}(\tilde{p}_\perp+\tilde{p}_\parallel)-\frac{(\tilde{p}_\perp+\tilde{p}_\parallel+\tilde{C})}{B}\frac{\partial B}{\partial r}-B\frac{d}{dr}\left(\frac{1}{B_{\max}}\right)2^{5/2}\pi m_h\left[\frac{B/2B_{\max}}{(1-B/B_{\max})^{1/2}}-\left(1-\frac{B}{B_{\max}}\right)^{1/2}\right]\int_0^\infty\mathscr{E}^{3/2}F_h\left(\mu=\frac{\mathscr{E}}{B_{\max}},\mathscr{E},r\right)d\mathscr{E}\right\}. \tag{82}$$

Further progress requires explicit expressions for $\tilde{p}_\perp(r,\theta)$, $\tilde{p}_\parallel(r,\theta)$, and $\tilde{C}(r,\theta)$. Recalling Eqs. (40), (42), and (49), the distribution function of the heated minority ions may be written

$$F_h=2n_hG(r)\left(\frac{m_h}{2\pi T_\perp}\right)^{3/2}\exp\left(-\frac{mv_\parallel^2}{2T_\parallel}-\frac{mv_\perp^2}{2T_R}\right), \tag{83}$$

where

$$\frac{1}{T_R(r,\theta)}=\frac{B_R}{B}\left(\frac{1}{T_\perp}-\frac{1}{T_\parallel}\right)+\frac{1}{T_\parallel}. \tag{84}$$

Substituting these expressions into Eqs. (74)–(76), and restricting the domain of integration to passing velocity space, we obtain

$$\tilde{p}_\parallel=\frac{6n_hGT_\parallel(T_\parallel/T_\perp)^{3/2}}{[\mu^{3/2}((B_{\max}/B)-1)^{3/2}+\mu^3]}\times\left[\left(\frac{B_{\max}}{B}-1\right)\mu+\frac{1}{3}\left(\frac{T_\parallel}{T_R}\right)^2\right], \tag{85}$$

$$\tilde{p}_\perp=\frac{2n_hGT_\perp(T_\parallel/T_\perp)^{5/2}[\mu-\frac{1}{4}((B_{\max}/B)-1)]}{\mu^{3/2}[\mu^{3/2}+\frac{3}{2}\mu((B_{\max}/B)-1)^{1/2}-\frac{1}{2}((B_{\max}/B)-1)^{3/2}]} \tag{86}$$

$$\tilde{C}=\frac{n_hGT_\parallel(T_\parallel/T_\perp)^{3/2}}{2\mu^{3/2}((B_{\max}/B)-1)^{1/2}}\frac{[((B_{\max}/B)-1)^{1/2}+3\mu^{1/2}]}{[((B_{\max}/B)-1)^{1/2}+\mu^{1/2}]^3}, \tag{87}$$

where

$$\mu=\frac{B_{\max}-B}{B}+\frac{T_\parallel}{T_R}. \tag{88}$$

We now turn to the expressions required in the final integral in Eq. (82). It follows from Eq. (3) that, to leading order in ϵ,

$$\frac{B/2B_{\max}}{(1-B/B_{\max})^{1/2}}+\left(1-\frac{B}{B_{\max}}\right)^{1/2}=\frac{1}{2}\left(\frac{R_0}{r}\right)^{1/2}\frac{1}{(1+\cos\theta)^{1/2}}, \tag{89}$$

$$\frac{d}{dr}\left(\frac{1}{B_{\max}}\right)=-\frac{B_0}{R_0B_{\max}^2}. \tag{90}$$

It follows from Eq. (83) that

$$2^{5/2}\pi m_h \int_0^\infty \mathscr{E}^{3/2} F_h\left(\mu=\frac{\mathscr{E}}{B_{\max}},\mathscr{E},r\right)d\mathscr{E}=3n_h(r)G(r)\left(\frac{T_B}{T_\perp}\right)^{3/2}T_B, \tag{91}$$

where

$$\frac{1}{T_B}=\frac{B_R}{B_{\max}}\left(\frac{1}{T_\perp}-\frac{1}{T_\parallel}\right)+\frac{1}{T_\parallel}=\frac{1}{T_R(r,\pi/2)}. \tag{92}$$

Using Eq. (3) and Eqs. (89)–(91), and integrating by parts where appropriate, Eq. (82) becomes

$$\begin{aligned}\delta W_{\rm hfp}=&\pi|\xi_{r0}|^2 r_1\oint d\theta\cos\theta[\tilde p_\perp(r_1,\theta)+\tilde p_\parallel(r_1,\theta)]-\pi|\xi_{r0}|^2\int_0^{r_1}dr\oint d\theta\cos\theta[\tilde p_\perp(r,\theta)+\tilde p_\parallel(r,\theta)]\\&+\frac{\pi|\xi_{r0}|^2}{R_0}\int_0^{r_1}r\,dr\oint d\theta\cos^2\theta[\tilde p_\perp(r,\theta)+\tilde p_\parallel(r,\theta)+\tilde C(r,\theta)]\\&+\frac{3\pi|\xi_{r0}|^2}{2R_0^{1/2}}\int_0^{r_1}r^{1/2}\,dr\oint d\theta\frac{\cos\theta}{(1+\cos\theta)^{1/2}}n_h(r)G(r)\left(\frac{T_B}{T_\perp}\right)^{3/2}T_B(r).\end{aligned} \tag{93}$$

Here, $\tilde p_\perp$, $\tilde p_\parallel$, and $\tilde C$ are defined by Eqs. (85)–(87), and the temperatures $T_\perp$, T_R, and T_B are defined by Eqs. (41), (84), and (92), respectively. We normalize the expression for $\delta W_{\rm hfp}$ with respect to W_0 defined by Eq. (58), yielding $(\delta W_{\rm hfp})_N$, and use the circumflex ($\hat{}$) to denote quantities normalized to 10^{19} m^{-3}, 1 keV, and 1 T as in Eqs. (60)–(62). We note, however, that the $\tilde C$ term, when expanded to leading order in ϵ and integrated over θ, contains a singularity which is exactly canceled by a singularity in the last term. It is therefore convenient to use the result

$$\int_0^{2\pi}\frac{\cos\theta\,d\theta}{(1+\cos\theta)^{1/2}}=-\int_0^{2\pi}\frac{\cos^2\theta\,d\theta}{(1+\cos\theta)^{1/2}}+\frac{4\sqrt{2}}{3}, \tag{94}$$

and to define

$$\begin{aligned}\hat C'\equiv&\hat C-\frac{3}{2x^{1/2}\epsilon_a^{1/2}(1+\cos\theta)^{1/2}}\hat n_h(x)G(x)\left(\frac{\hat T_B}{\hat T_\perp}\right)^{3/2}\hat T_B(x)\\=&\frac{3}{2}\hat n_h(x)G(x)\left(\frac{\hat T_B}{\hat T_\perp}\right)^{3/2}\hat T_B(x)\left\{\frac{1}{3}\frac{\hat T_\parallel}{\hat T_B}-3\frac{\hat T_\parallel}{\hat T_B}[1+\epsilon_a x(1+\cos\theta)]^{5/2}+\epsilon_a^{1/2}x^{1/2}(1+\cos\theta)^{1/2}\right.\\&\times\left[\frac{(\hat T_\parallel/\hat T_B)^{3/2}}{[1+\epsilon_a x(1+\cos\theta)]^{1/2}+1}-3\left(\frac{\hat T_\parallel}{\hat T_B}\right)^{3/2}-3\left(\frac{\hat T_\parallel}{\hat T_B}\right)^{1/2}[1+\epsilon_a x(1+\cos\theta)]^2\right]\\&-\epsilon_a x(1+\cos\theta)[1+\epsilon_a x(1+\cos\theta)]^{3/2}\\&\left.-3\left(\frac{\hat T_\parallel}{\hat T_B}\right)^{3/2}\epsilon_a^{3/2}x^{3/2}(1+\cos\theta)^{3/2}-\left(\frac{\hat T_\parallel}{\hat T_B}\right)^{3/2}\epsilon_a^{5/2}x^{5/2}(1+\cos\theta)^{5/2}\right\}\\&\times[1+\epsilon_a x(1+\cos\theta)]^{-3/2}\left[\epsilon_a^{1/2}x^{1/2}(1+\cos\theta)^{1/2}+\left(\frac{\hat T_\parallel}{\hat T_B}\right)^{1/2}[1+\epsilon_a x(1+\cos\theta)]^{1/2}\right]^{-3}.\end{aligned} \tag{95}$$

The dimensionless form of Eq. (93) then becomes

$$\begin{aligned}(\delta W_{\rm hfp})_N=&1.068\times10^{-4}\frac{\epsilon_a^{-3}x_1^{-3}}{\hat B_0^2}\left[\int_0^{2\pi}d\theta\cos\theta[\hat p_\perp(x_1,\theta)+\hat p_\parallel(x_1,\theta)]-\frac{1}{x_1}\int_0^{x_1}dx\int_0^{2\pi}d\theta\cos\theta[\hat p_\perp(x,\theta)+\hat p_\parallel(x,\theta)]\right.\\&\left.+\frac{\epsilon_a}{x_1}\int_0^{x_1}x\,dx\int_0^{2\pi}d\theta\cos^2\theta[\hat p_\perp(x_1,\theta)+\hat p_\parallel(x_1,\theta)+\hat C'(x,\theta)]+\frac{2\sqrt{2}\epsilon_a^{1/2}}{x_1}\int_0^{x_1}x^{1/2}\,dx\,\hat n_h(x)G(x)\left(\frac{\hat T_B}{\hat T_\perp}\right)^{3/2}\hat T_B(x)\right],\end{aligned} \tag{96}$$

where $\hat p_\parallel(x,\theta)$ and $\hat p_\perp(x,\theta)$ are given by the dimensionless form of Eqs. (85) and (86), with $\mu=x\epsilon_a(1+\cos\theta)+\hat T_\parallel/\hat T_R$ and $B_{\max}/B-1=x\epsilon_a(1+\cos\theta)$. Equation (96) contains no singularities, and is therefore convenient for numerical computation.

VI. NUMERICAL RESULTS

The key expressions derived in the preceding sections give formulas for $\delta W_{\rm ht}$ and $\delta W_{\rm hfp}$ which are directly parametrized by quantities such as P_0, Δ, and δ which describe the

RF power deposition among the minority ions. These expressions must be evaluated numerically: Table I gives a complete list of the parameters which must be specified for this purpose. It is clear that a wide range of stability studies is possible. However, in some cases the parametric dependence is very simple. For example, the various components of the hot-ion contribution to δW all scale linearly with $T_\perp$, and hence with the RF power level [see Eq. (69)]. Also, it is apparent from Eqs. (66), (67), (69), (95), and (96) that $\delta W_{\rm ht}$ and $\delta W_{\rm hfp}$ are independent of n_{h0}/n_0. This follows from the Stix model [Eq. (10)], which implies that the total energy transferred via ion cyclotron resonance to the minority ions depends only on the RF power input.

We concentrate on the case of ^{3}He minority ions ($A_h=3$, $Z_h=2$), and an RF power deposition profile which is centered on the magnetic axis ($\hat{\epsilon}=0$), with a vertical spread $\Delta=20$ cm[11] (when $\hat{\epsilon}=0$, the value of δ is irrelevant). Appropriate values for many of the other parameters can be found in Ref. 11: we set $P_c=5-20$ MW, $n_0=n_{e0}=2\times10^{19}$ m^{-3}, $\nu_n=\nu_{ne}=0.5$, $T_{e0}=10$ keV, $\nu_{T_e}=1$, $a=1.2$ m, $R_0=3.1$ m, and $B_0=3.3$ T. Our numerical results illustrate the effects of varying the four remaining parameters: α_T, q_0, λ, and ν. Unless otherwise stated, $\alpha_T=0.1$, $q_0=0.7$, $\lambda=2$, and $\nu=1$. Our benchmark q profile is thus parabolic, with $r_1\simeq0.46a$. Observed values of r_1/a in JET can be as high as 0.6 in the case of H-mode monster sawteeth.[18] Accordingly, q_0, λ, and ν can be varied such that r_1/a takes any value in the range 0–0.6, although the value of q_0 is also constrained by the requirement that $|q-1|\ll1$ inside the $q=1$ surface.

Figure 1 shows the real and imaginary parts of $(\delta W_{\rm ht})_N$ (curves A and B), $(\delta W_{\rm hfp})_N$ (curve C), and the sum $\mathrm{Re}(\delta W_{\rm ht})_N+(\delta W_{\rm hfp})_N$ (curve D), as functions of α_T: the RF power is 20 MW, and $T_\perp(0)\simeq1.3$ MeV. The hot-ion contribution to δW is predominantly real, and we invariably find that $\mathrm{Re}(\delta W_{\rm ht})_N+(\delta W_{\rm hfp})_N>0$, i.e., the hot ions have a stabilizing effect. The total hot-ion plasma energy is almost

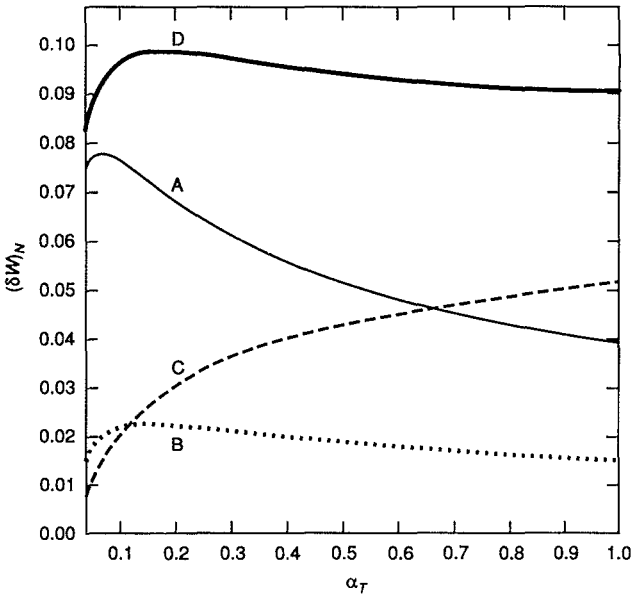

FIG. 1. Real and imaginary parts of $(\delta W_{\rm ht})_N$ (curves A and B), $(\delta W_{\rm hfp})_N$ (curve C), and the sum $\mathrm{Re}(\delta W_{\rm ht})_N+(\delta W_{\rm hfp})_N$ (curve D), as functions of α_T. The RF power is 20 MW: the other parameters are given in the text.

independent of α_T, except when this parameter is less than about 0.1. If F_h is highly anisotropic, the dominant contribution to $\delta W_{\rm hot}$ comes, as expected, from trapped ions. The passing ion component increases rapidly with α_T, becoming dominant as F_h approaches isotropy.

In Fig. 2, $\mathrm{Re}(\delta W_{\rm ht})_N+(\delta W_{\rm hfp})_N$ is plotted as a function of α_T for $P_c=5$ MW, 10 MW, and 20 MW: this shows explicitly the linear dependence on P_c mentioned above. We noted in Sec. IV that stability requires the hot-ion component of $(\delta W)_N$ to exceed $|(13/144-\beta_p^2)(1-q_0)|$, where β_p is

TABLE I. Complete set of parameters required to specify $(\delta W_{\rm ht})_N$ and $(\delta W_{\rm hfp})_N$.

	Name	Units
$q=q_0[1+\lambda(r/a)^{2\nu}]^{1/\nu}$	q_0	
	λ	
	ν	
$n_h=(n_{h0}/n_0)n_0[1-(r/a)^2]^{\nu_n}$	n_{h0}/n_0	
	n_0	10^{19} m^{-3}
	ν_n	
$T_\perp$ (see Sec. II)	A_h	atomic mass units
	Z_h	
	P_c	MW
	Δ	m
	δ	m
$n_e=n_{e0}[1-(r/a)^2]^{\nu_{ne}}$	n_{e0}	10^{19} m^{-3}
	ν_{ne}	
$T_e=T_{e0}[1-(r/a)^2]^{\nu_{T_e}}$	T_{e0}	keV
	ν_{T_e}	
$T_\parallel=\alpha_T T_\perp$	α_T	
Minor and major radius	a, R_0	m
Central magnetic field	B	T
$\hat{\epsilon}\equiv(R_{\rm res}-R_0)/R_0$		

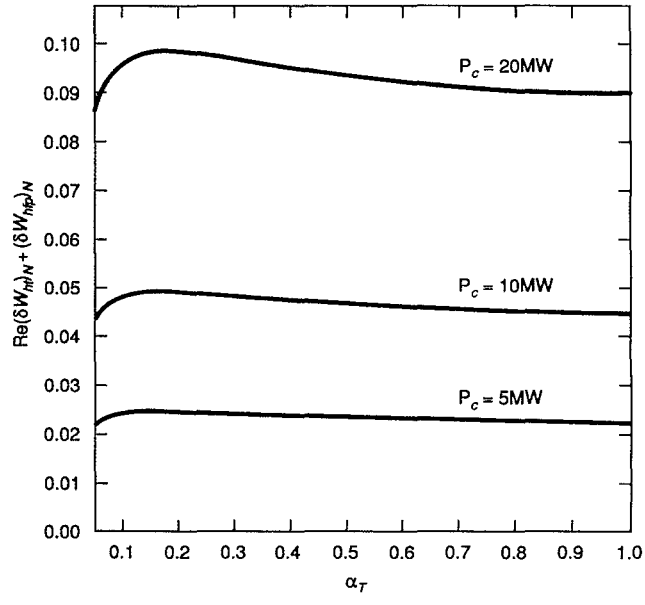

FIG. 2. $\mathrm{Re}(\delta W_{\rm ht})_N+(\delta W_{\rm hfp})_N$ as a function of α_T for three values of P_c.

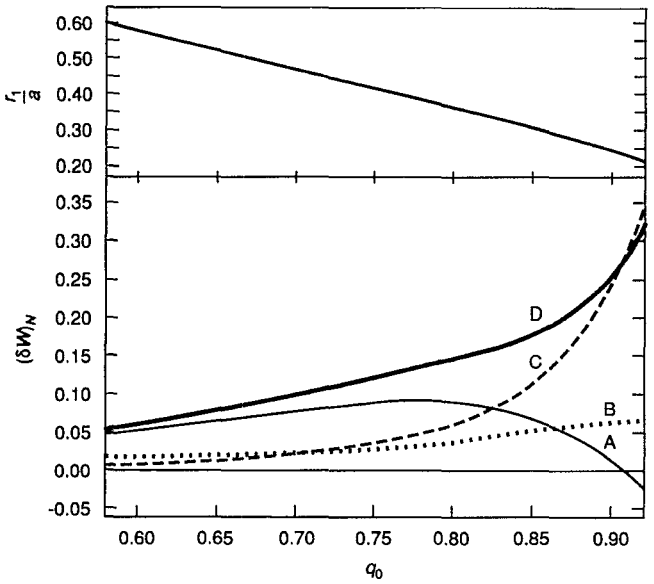

FIG. 3. Lower frame: as Fig. 1 except that $(\delta W_{\rm ht})_N$ and $(\delta W_{\rm hfp})_N$ are plotted as functions of q_0. Upper frame: r_1/a as a function of q_0.

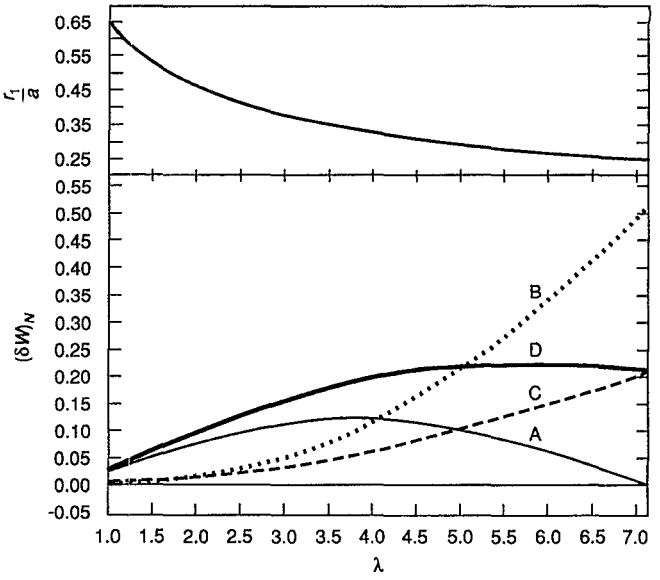

FIG. 4. As Fig. 3 except that $(\delta W_{\rm ht})_N$, $(\delta W_{\rm hfp})_N$, and r_1/a are plotted as functions of λ.

the total poloidal plasma beta at the $q=1$ surface. However, this statement is based on the implicit assumption that the fluid pressure in the plasma core is isotropic, so that β_p is uniquely defined. In fact, for realistic values of n_{h0}/n_0 and RF powers in the 5–20 MW range, the pressure in the plasma core contains a significant contribution from the (highly anisotropic) minority ions, and so, in the parameter regime which is relevant to ICRH experiments, Eq. (57) is not strictly valid, and a precise comparison between $\delta W_{\rm ht}+\delta W_{\rm hfp}$ and $\delta W^{(T)}$ is not possible. If, however, we assume that Eq. (57) is approximately correct, we can infer that the hot-ion contribution to δW will stabilize the $m=1$ internal kink if

$$\beta_p \lesssim \left(\frac{13}{144}+\frac{1}{1-q_0}[{\rm Re}(\delta W_{\rm hot})_N+(\delta W_{\rm hfp})_N]\right)^{1/2}. \quad (97)$$

In terms of the results presented in Fig. 2, the marginally stable value of β_p lies in the range 0.4–0.65, depending on the values of α_T and P_c: in the MHD limit, the critical value of β_p is $(13/144)^{1/2}\simeq 0.3$. Stable values of β_p well in excess of the MHD threshold thus exist.

We now proceed to examine the effects of varying the q profile, subject to the constraint that $r_1 \lesssim 0.6a$. The lower frames of Figs. 3–5 show $(\delta W_{\rm ht})_N$ and $(\delta W_{\rm hfp})_N$ as functions of q_0, λ, and ν, respectively (see Table I): the upper frames show the radius of the $q=1$ surface. In each case, the total real contribution to $(\delta W_{\rm hot})_N$ tends to increase as r_1/a is reduced, and for $r_1 \lesssim 0.3a$ the stabilizing effect of passing ions is again dominant. When $r_1 \simeq 0.3a$, the marginally stable value of β_p indicated by Eq. (97) is about 1.0, irrespective of the q-profile parameters. We find as $r_1 \to 0$ that $(\delta W_{\rm hfp})_N$ increases monotonically, whereas the real and imaginary parts of $(\delta W_{\rm ht})_N$ both tend to zero.

Since, in the MHD limit, the growth rate of the $m=1$ internal kink is proportional to the negative of the total plasma energy,[19] the existence of an imaginary part of $\delta W_{\rm ht}$ implies a finite real frequency ω, and self-consistency requires that $\omega \ll \langle \omega_{dh} \rangle$ for the majority of hot ions, whose pitch angles do not correspond to values of k^2 lying close to k_c^2. In terms of $(\delta W)_N$, the growth rate obtained in Ref. 19 can be written as

$$\gamma = -\frac{3\pi}{4}\frac{r_1}{R_0^3}\frac{v_{\rm A}}{q'}(\delta W)_N, \quad (98)$$

where the Alfvén speed $v_{\rm A}$ and $q' \equiv dq/dr$ are both evaluated at $r=r_1$ (note that the quantity $\delta W_{\rm min}$ defined in Ref. 19

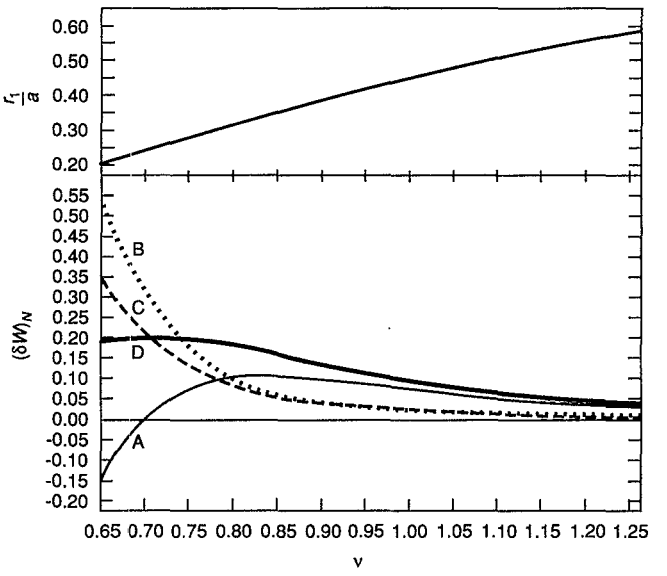

FIG. 5. As Fig. 3 except that $(\delta W_{\rm ht})_N$, $(\delta W_{\rm hfp})_N$, and r_1/a are plotted as functions of ν.

is the energy per unit toroidal length). Using the fact that $q'=2(1-q_0)/r_1$ in the case of a parabolic q profile, we infer that

$$\omega=\frac{3\pi}{8}\frac{r_1^2}{R_0^3}\frac{v_A}{1-q_0}\,\mathrm{Im}(\delta W_{ht})_N. \tag{99}$$

The modulus of the bounce-averaged toroidal precessional drift frequency is given by[20]

$$|\langle\omega_{dh}\rangle|=\frac{|2E(k^2)-K(k^2)|\mathscr{E}q}{K(k^2)\Omega_h r R_0}\sim\frac{\mathscr{E}}{\Omega_h r_1 R_0}, \tag{100}$$

where Ω_h is the minority ion cyclotron frequency, and the order-of-magnitude approximation is valid for ions with $k^2\neq k_c^2$. We thus have

$$\frac{\omega}{|\langle\omega_{dh}\rangle|}\sim\frac{3\pi}{8}(x_1\epsilon_a)^3\frac{v_A\Omega_h R_0}{\mathscr{E}(1-q_0)}\,\mathrm{Im}(\delta W_{ht})_N. \tag{101}$$

Adopting the model parameters used to obtain Figs. 1–5, and setting $m_h\mathscr{E}=T_\perp(0)\sim 1$ MeV, we find that $\omega/|\langle\omega_{dh}\rangle|$ is typically less than about 0.1. In fact, for any realistic set of q-profile and RF power input parameters, one can self-consistently take the low-frequency limit in Eq. (1).

Internal kink perturbations with $\omega\sim\langle\omega_{dh}\rangle$ are widely believed to be associated with so-called fishbone oscillations.[5] In a future paper we will extend our stability analysis of the model distribution given by Eq. (40) to the case of mode frequencies which are not small compared to $\langle\omega_{dh}\rangle$. One additional complication arising from finite ω is that the energy integrals in δW_{hot} are no longer expressible in terms of Γ functions, and in fact must be evaluated numerically when F_h is given by Eq. (40). A review of theoretical work on finite frequency $m=1$ modes can be found in Ref. 9. The excitation of fishbones has been variously attributed to spatial gradients in the minority ion population,[5] bulk ion pressure gradients,[21] and combinations of these.[22] In any event, it is likely that deeply trapped particles have a destabilizing effect on wave modes with $\omega\sim\langle\omega_{dh}\rangle$,[20] and so one of the aims of our fishbone stability analysis will be to determine the effect of varying the anisotropy parameter α_T. Passing minority ions do not contribute to the kinetic (frequency-dependent) term in Eq. (1), and therefore our expression for δW_{hfp} is valid for all values of ω. Equation (98) applies whenever the modulus of the complex wave frequency greatly exceeds the bulk ion diamagnetic frequency. In such cases, passing minority ions always have a stabilizing effect, irrespective of ω, since δW_{hfp} is positive definite (see Figs. 1 and 3–5). Any study of fishbone modes based on Eq. (40) must therefore take into account the stabilizing effect of passing minority ions, as well as the (possibly destabilizing) effect of trapped ions.

It is appropriate at this stage to compare our results with those obtained in Ref. 23, which were applied to the case of on-axis ICRH in the Tore Supra tokamak.[24] It was concluded in Ref. 23 that passing minority ions have a greater stabilizing effect than trapped ions. Using q-profile parameters, RF deposition parameters and hot-ion anisotropy parameters appropriate for ICRH experiments in Tore Supra, we find that our model also yields the result $(\delta W_{hfp})_N>\mathrm{Re}(\delta W_{ht})_N$, although the ratio of these two quantities is rather sensitive to the precise value adopted for the vertical spread of the RF power deposition (Δ). This qualitative agreement occurs despite the fact that the model adopted in Ref. 23 for the minority ion distribution function, proposed originally by Bécoulet and co-workers,[25] differs significantly from that adopted here, in terms of both velocity space structure and radial profile. In particular, the minority ion distribution in Ref. 23 is identically zero for $\lambda\leq B_R^{-1}$, i.e., it is assumed that there are no deeply trapped heated ions. In the model adopted in this paper, which is motivated by the Stix model interpretation of JET ICRH experiments[11] and related Fokker–Planck studies,[14,15] deeply trapped ions make a significant contribution to $\mathrm{Re}(\delta W_{ht})_N$, thus augmenting the ratio $\mathrm{Re}(\delta W_{ht})_N/(\delta W_{hfp})_N$.

VII. CONCLUSIONS

We have used a generalized energy principle to examine the stabilizing effect of ion cyclotron resonant heating (ICRH) on zero frequency $m=1$ internal kink displacements, which are associated with sawtooth oscillations. Simple expressions, consisting of one-dimensional and two-dimensional integrals, have been obtained for the contribution to the plasma energy δW of an ICRH-heated minority ion population. Both trapped and passing ions have been taken into account. The model minority ion distribution function is based on Stix's model, and, when expressed as a function of energy, magnetic moment, and minor radius, is independent of poloidal angle, thereby satisfying the Vlasov equation. The perpendicular temperature is specified as a function of minor radius in terms of the total RF power P_c and its deposition profile. A consequence of Stix's model is that the minority ion component of the plasma energy has a simple linear dependence on P_c, and we have shown numerically that it is also insensitive to the anisotropy parameter $T_\parallel/T_\perp$. Our treatment includes an imaginary contribution to the plasma energy, arising from the zero-frequency Landau resonance of heated ions near the trapped–passing boundary: the existence of this imaginary contribution implies a finite mode frequency, which is typically much smaller than the toroidal precessional drift frequency of the minority ions. Using parameters inferred from ICRH experiments in JET, we have shown that the ideal $m=1$ internal kink mode can be stable when β_p is of the order of unity—well above the MHD instability threshold value of 0.3. Both trapped and passing minority ions contribute to $m=1$ internal kink stabilization, with trapped ions making the greater contribution if $T_\perp/T_\parallel\gtrsim 10$ and the radius of the $q=1$ surface $r_1\gtrsim 0.3a$. The computed values of the normalized plasma energy depend on the q profile, and above all on the value of r_1: minority ion stabilization is most easily achieved if r_1/a is small.

ACKNOWLEDGMENTS

We are grateful to Dr. L.-G. Eriksson and Dr. A. Thyagaraja for helpful discussions regarding ICRH-heated ion distributions and q-profile measurements, respectively.

This work was funded jointly by the United Kingdom Department of Trade and Industry and Euratom.

APPENDIX: NORMALIZATION OF HOT ION DISTRIBUTION

The function $G(r)$, which appears in the expression for the minority ion distribution function [Eq. (49)], may be evaluated as follows. As a first step, we divide the domain of integration in Eq. (50) into passing and trapped regions:

$$\int_0^{1/B_{\min}} d\lambda \oint d\theta = \int_0^{1/B_{\max}} d\lambda \int_0^{2\pi} d\theta + \int_{1/B_{\max}}^{1/B_{\min}} d\lambda \int_{-\theta_b}^{\theta_b} d\theta. \tag{A1}$$

Next, following Eq. (3), we may write

$$1-\lambda B(r,\theta) = 1-\lambda B_0+\lambda B_0\epsilon[1-2\sin^2(\theta/2)]$$
$$= [1-\lambda B_0(1-\epsilon)](1-\hat{k}^2\sin^2\phi), \tag{A2}$$

where $\phi=\theta/2$ and

$$\hat{k}^2 = 2\lambda B_0\epsilon/[1-\lambda B_0(1-\epsilon)]. \tag{A3}$$

Defining $\hat{k}^2\sin^2\phi=\sin^2 u$, it follows that to leading order we may write

$$\frac{1}{2\pi}\int_{-\theta_b}^{\theta_b}\frac{B(r,\theta)d\theta}{[1-\lambda B(r,\theta)]^{1/2}}$$
$$= \frac{2B_0}{\pi}\frac{1}{[1-\lambda B_0(1-\epsilon)]^{1/2}}\frac{1}{\hat{k}}$$
$$\times\int_0^{\pi/2}\left(1-\frac{1}{\hat{k}^2}\sin^2 u\right)^{-1/2} du$$
$$= \frac{2B_0\tilde{k}}{\pi[1-\lambda B_0(1-\epsilon)]^{1/2}}K(\tilde{k}^2), \tag{A4}$$

where $\tilde{k}^2=1/\hat{k}^2$ and we have used Eq. (14). It follows from Eq. (A3) that $\lambda B_0[1+\epsilon(2\tilde{k}^2-1)]=1$, and hence

$$1-\lambda B_0(1-\epsilon) = 2\epsilon\tilde{k}^2/[1+\epsilon(2\tilde{k}^2-1)]; \tag{A5}$$

then using this expression in Eq. (A4) we recover to leading order,

$$\frac{1}{2\pi}\int_{-\theta_b}^{\theta_b}\frac{B(r,\theta)d\theta}{[1-\lambda B(r,\theta)]^{1/2}} \simeq \frac{2}{\pi}\frac{B_0}{(2\epsilon)^{1/2}}K(\tilde{k}^2). \tag{A6}$$

Next we turn to the first component of the integrand in Eq. (50), still focusing on the trapped part of the integration domain, as identified in Eq. (A1). It follows from Eq. (42) and the definition of variables leading to Eq. (A5) that

$$\lambda B_R+\frac{T_\perp}{T_\parallel}|1-\lambda B_R| = \frac{1-\hat{\epsilon}+(T_\perp/T_\parallel)|\hat{\epsilon}+\epsilon(2\tilde{k}^2-1)|}{1+\epsilon(2\tilde{k}^2-1)}. \tag{A7}$$

The end points of the trapped pitch-angle integration at $B_{\min}^{-1}$ and $B_{\max}^{-1}$ correspond by Eq. (3) to $\lambda B_0=(1-\epsilon)^{-1}$ and $(1+\epsilon)^{-1}$, respectively, and hence to $\tilde{k}=0$ and 1, respectively. Also, it follows from the definition of $\tilde{k}^2$ that

$$B_0\, d\lambda = -\frac{4\epsilon\tilde{k}\, d\tilde{k}}{[1+\epsilon(2\tilde{k}^2-1)]^2}. \tag{A8}$$

Thus we may combine Eqs. (A6)–(A8) to express the trapped integral from Eqs. (50) and (A1) in the form

$$I_t \equiv \int_{1/B_{\max}}^{1/B_{\min}}\frac{d\lambda}{[\lambda B_R+(T_\perp/T_\parallel)|1-\lambda B_R|]^{3/2}}\frac{1}{2\pi}$$
$$\times\int_{-\theta_b}^{\theta_b}\frac{B\, d\theta}{(1-\lambda B)^{1/2}} = \frac{4}{\pi}(2\epsilon)^{1/2}$$
$$\times\int_0^1\frac{k\, dk\, K(k^2)}{[1-\hat{\epsilon}+(T_\perp/T_\parallel)|\hat{\epsilon}+\epsilon(2k^2-1)|]^{3/2}}+O(\epsilon). \tag{A9}$$

The correction $O(\epsilon)$ in Eq. (A9) arises both from the neglect of $O(\epsilon)$ in forming the numerator when obtaining Eq. (A4), and from the factor $[1+\epsilon(2k^2-1)]^{-1/2}$ that arises from combining the $-3/2$ power of Eq. (A9) with Eq. (A8). In the denominator of Eq. (A9), ϵ survives because it is multiplied by $T_\perp/T_\parallel$, which may be a large factor.

Let us now turn to the passing domain specified in Eq. (A1). Referring back to Eqs. (3), (A2), and (A3),

$$\frac{1}{2\pi}\int_0^{2\pi}\frac{B(r,\theta)d\theta}{[1-\lambda B(r,\theta)]^{1/2}}$$
$$= \frac{2B_0}{\pi}\int_0^{\pi/2}\frac{d\theta}{[1-\hat{k}^2\sin^2(\theta/2)]^{1/2}}\frac{1}{[1-\lambda B_0(1-\epsilon)]^{1/2}}$$
$$= \frac{K(\hat{k}^2)}{[1-\lambda B_0(1-\epsilon)]^{1/2}}. \tag{A10}$$

It follows from Eq. (A3) that $\lambda B_0[\hat{k}^2+\epsilon(2-\hat{k}^2)]/\hat{k}^2=1$, so that the end points of the passing pitch-angle integration at $\lambda B_0=0$ and $(1+\epsilon)^{-1}$ correspond to $\hat{k}^2=0$ and 1, respectively. Also, we have

$$1-\lambda B_0(1-\epsilon) = 2\epsilon/[\hat{k}^2+\epsilon(2-\hat{k}^2)], \tag{A11}$$

so that Eq. (A10) becomes

$$\frac{1}{2\pi}\int_0^{2\pi}\frac{B(r,\theta)d\theta}{[1-\lambda B(r,\theta)]^{1/2}}$$
$$= \frac{2}{\pi}\frac{B_0}{(2\epsilon)^{1/2}}[\hat{k}^2+\epsilon(2-\hat{k}^2)]^{1/2}K(\hat{k}^2). \tag{A12}$$

From Eq. (A11) we also obtain

$$B_0\, d\lambda = \frac{4\epsilon\hat{k}\, d\hat{k}}{[\hat{k}^2+\epsilon(2-\hat{k}^2)]^2}. \tag{A13}$$

In considering the first component of the integrand in Eq. (50), we may again use Eq. (A7), this time noting that $\tilde{k}^2=1/\hat{k}^2$. Together with Eqs. (A12) and (A13), this yields

$$I_p \equiv \int_0^{1/B_{\max}}\frac{d\lambda}{[\lambda B_R+(T_\perp/T_\parallel)|1-\lambda B_R|]^{3/2}}\int_0^{2\pi}\frac{B\, d\theta}{(1-\lambda B)^{1/2}}$$
$$= \frac{4}{\pi}(2\epsilon)^{1/2}\int_0^1\frac{k\, dk\, K(k^2)}{[(1-\hat{\epsilon})k^2+(T_\perp/T_\parallel)|\hat{\epsilon}k^2+\epsilon(2-k^2)|]^{3/2}}. \tag{A14}$$

Combining Eqs. (A9) and (A14), we have

$$I_t+I_p=\frac{2}{\pi}(2\epsilon)^{1/2}\int_0^1 dk^2\ K(k^2)$$
$$\times\left[\left(1-\hat{\epsilon}+\frac{T_\perp}{T_\parallel}|\hat{\epsilon}+\epsilon(2k^2-1)|\right)^{-3/2}\right.$$
$$\left.+\left((1-\hat{\epsilon})k^2+\frac{T_\perp}{T_\parallel}|\hat{\epsilon}k^2+\epsilon(2-k^2)|\right)^{-3/2}\right]. \quad \text{(A15)}$$

From the definitions of I_t and I_p it is clear that

$$G(r)=(I_t+I_p)^{-1}, \quad \text{(A16)}$$

and so the integral in Eq. (A15) determines the normalization factor in our expression for the heated minority ion distribution.

[1]D. J. Campbell, D. F. H. Start, J. A. Wesson, C. V. Bartlett, V. P. Bhatnagar, M. Bures, J. G. Cordey, G. A. Cottrell, P. A. Dupperex, A. W. Edwards, C. D. Challis, C. Gormezano, C. W. Gowers, R. S. Granetz, H. Hamnen, T. Hellsten, J. Jacquinot, E. Lazzaro, P. J. Lomas, N. Lopes Cardozo, P. Mantica, J. A. Snipes, D. Stork, P. E. Stott, P. R. Thomas, E. Thompson, K. Thomsen, and G. Tonetti, Phys. Rev. Lett. **60**, 2148 (1988).

[2]T. M. Antonsen and Y. C. Lee, Phys. Fluids **25**, 132 (1982).

[3]J. B. Taylor and R. J. Hastie, Phys. Fluids **8**, 323 (1965).

[4]M. D. Kruskal and C. R. Oberman, Phys. Fluids **1**, 275 (1958).

[5]L. Chen, R. B. White, and M. N. Rosenbluth, Phys. Rev. Lett. **52**, 1122 (1984).

[6]J. W. Van Dam, M. N. Rosenbluth, and Y. C. Lee, Phys. Fluids **25**, 1349 (1982).

[7]B. Coppi, R. J. Hastie, S. Migliuolo, F. Pegoraro, and F. Porcelli, Phys. Lett. A **132**, 267 (1988).

[8]B. Coppi, S. Migliuolo, F. Pegoraro, and F. Porcelli, Phys. Fluids B **2**, 927 (1990).

[9]F. Porcelli, Plasma Phys. Controlled Fusion **33**, 1601 (1991).

[10]T. H. Stix, Nucl. Fusion **15**, 737 (1975).

[11]D. A. Boyd, D. J. Campbell, J. G. Cordey, W. G. F. Core, J. P. Christiansen, G. A. Cottrell, L.-G. Eriksson, T. Hellsten, J. J. Jacquinot, O. N. Jarvis, S. E. Kissel, C. Lowrey, P. Nielsen, G. Sadler, D. F. H. Start, P. R. Thomas, P. Van Belle, and J. A. Wesson, Nucl. Fusion **29**, 593 (1989).

[12]G. A. Cottrell and D. F. H. Start, Nucl. Fusion **31**, 61 (1991).

[13]F. Pegoraro, F. Porcelli, B. Coppi, P. Detragiache, and S. Migliuolo, in *Plasma Physics and Controlled Nuclear Fusion Research, 1988* (International Atomic Energy Agency, Vienna, 1989), Vol. 2, p. 243.

[14]G. D. Kerbel, and M. G. McCoy, Phys. Fluids **28**, 3629 (1985).

[15]R. W. Harvey, M. G. McCoy, G. D. Kerbel, and S. C. Chiu, Nucl. Fusion **26**, 43 (1986).

[16]L. Villard, L. Appert, R. Gruber, and J. Vaclavik, Comput. Phys. Rep. **4**, 95 (1986).

[17]M. N. Bussac, R. Pellat, D. Edery, and J. L. Soulé, Phys. Rev. Lett. **35**, 1638 (1975).

[18]D. Pearson, D. J. Campbell, A. W. Edwards, and J. O'Rourke, in *Proceedings of the 18th European Conference on Controlled Fusion and Plasma Physics*, Berlin, Germany, 1991, edited by P. Baschmann and D. C. Robinson (European Physical Society, Petit-Lancy, Switzerland, 1991), Part II, Vol. 15C, p. 25.

[19]G. Ara, B. Basu, B. Coppi, G. Laval, M. N. Rosenbluth, and P. Rutherford, Ann. Phys. **112**, 443 (1978).

[20]R. B. White, L. Chen, F. Romanelli, and R. Hay, Phys. Fluids **28**, 278 (1985).

[21]B. Coppi and F. Porcelli, Phys. Rev. Lett. **57**, 2272 (1986).

[22]B. Coppi, P. Detragiache, S. Migliuolo, F. Pegoraro, and F. Porcelli, Phys. Rev. Lett. **63**, 2733 (1989).

[23]M. Zabiégo, X. Garbet, A. Bécoulet, F. Nguyen, and B. Saoutic, Nucl. Fusion **34**, 1489 (1994).

[24]B. Saoutic, M. Zabiégo, G. T. Hoang, A. Bécoulet, X. Garbet, T. Hutter, E. Joffrin, F. Nguyen, A. Samain, B. Beaumont, M. Goniche, L. Guiziou, H. Kuus, D. Moreau, A. L. Pecquet, G. Rey, and D. van Houtte, in *Proceedings of the 20th EPS Conference on Controlled Fusion and Plasma Physics*, Lisbon, Portugal, 1993, edited by J. A. Costa Cabral, M. E. Manso, F. M. Serra, and F. C. Schüller (European Physical Society, Petit-Lancy, Switzerland, 1993), Part I, Vol. 17C, p. 219.

[25]A. Bécoulet, D. J. Gambier, and A. Samain, Phys. Fluids B **3**, 137 (1991).